Biomechanical Responses of a New Neck For THOR-AV 5th Percentile Female Dummy

Z. Jerry Wang, Brian H. Loeber, Angela Tesny, Yun Seok Kang

Abstract A new neck was developed for the THOR-AV 5th percentile female dummy. The neck design followed the same concept as the THOR-AV 50th percentile male neck design and complied with the 5th percentile female neck anthropometry specifications. Prototype necks were built for biofidelity evaluations in six test conditions, covering the frontal, lateral, oblique and torsion responses. The neck frontal response has BioRank scores of 1.26 and 1.60 for Thunnissen et al. and Kang et al. test conditions respectively, both corresponding to *good* biofidelity. The neck lateral response has a BioRank scores of 2.39 and 1.65 for Wismans et al. and Kang et al. test conditions, corresponding to *marginal* and *good* biofidelity respectively. The neck oblique and torsion responses both have a BioRank score of 2.77 and 2.08 respectively, corresponding to *marginal* biofidelity. The overall biofidelity of the neck is *good* with a BioRank score of 1.96.

Keywords biofidelity, female, neck, THOR, THOR-AV 5F

I. INTRODUCTION

Anthropomorphic test devices (ATD) have been used to evaluate the performance of occupant restraint systems in automotive safety research for a few decades. The human neck is a critical and very complex component, and it plays a crucial role in protecting the head during a crash. ATD neck design has been challenging and the design has been evolving for decades with the advances of biomechanics research in human neck mechanical response. Hybrid I/II dummy neck was developed in 1971 with a molded rubber piece, which is repeatable, durable but non-biomechanical in its response characteristics [1]. Hybrid III neck was developed in 1976 with biomechanical bending and damping responses in both flexion and extension, which were based on responses of human volunteers by Mertz et al. [2]. The responses were focused on bending moment and head rotation relative to the torso in flexion and extension directions. However, the kinematics of the head and neck were not specified in Mertz's requirements. Thunnissen et al. [3] and Wismans et al. [4] analyzed the Naval Biodynamics Laboratory (NDBL) volunteer sled test data conducted in 1970s and recommended kinematics responses in frontal and lateral impact conditions for ATD neck design. However, it has been a challenge to achieve the T1 pulse for ATD evaluation though the sled pulse matches the NDBL volunteer test. Without matching the T1 pulse, the evaluation of the neck responses was in question. Wang et al. [5][6] presented a mini-sled, E-Liner Dummy Cert Sled (Humanetics, Farmington Hills, Michigan, USA) that has the capability of programming any sled pulse. The E-Liner Dummy Cert Sled can generate a T1 pulse exactly and allow to evaluate the neck biofidelity with the head and neck subsystem alone. Kang et al. [7] conducted PMHS head and neck on an impact sled and provided kinematics guidelines for ATD neck design. Biomechanical data of post motion human subjects (PMHS) or volunteers in six test conditions were available for the neck biofidelity evaluation[3][4][7], covering frontal [3][7], lateral [4][7], oblique and torsion [7] impact responses. The details of these six test conditions were outlined in [6] for 50th percentile male neck biofidelity evaluation. In the study [6], it demonstrated that the THOR-AV neck has a simpler design, a more representative anthropometry and a better biofidelity than the necks of THOR and Hybrid III 50th dummies.

THOR-5F neck was developed in recent years [5][8]. The frontal and rear cables inherited the complexity of a frontal and lateral cable system of the THOR-50M neck design. The complexity of the design poses challenges in dummy certification tests and compromises the durability and repeatability of the neck. Wang et al. [6] demonstrated that the THOR-AV 50M neck has a simpler design but superior biofidelity over the necks of THOR

Dr. Z. Jerry Wang is the Chief Technology Officer (phone +1 248 778 2133, email: jwang@humaneticsatd.com), Mr. Brian H. Loeber is a test engineer, both at Humanetics Innovative Solutions. Dr. Angela Tesny is a research scientist, and Dr. Yun Seok Kang is an associate professor, both at the Injury Biomechanics Research Center of The Ohio State University.

and Hybrid III 50th percentile dummies, especially in its torsion responses because of the introduction of a torsion element in its design. In lieu of the same concept, a THOR-AV 5th percentile female dummy (THOR-AV 5F) was designed. The new neck was evaluated in the six test conditions mentioned above, including two that were used to evaluate the THOR-5F neck design. The aim of the THOR-AV 5F neck development is to have a simpler design but an equal or better biofidelity than THOR-5F neck. A simpler neck design could improve its durability and repeatability.

Even though the THOR-AV 5F neck was designed in a similar concept to THOR-AV 50M neck. The dimension and geometry were in accordance with the 5th percentile female anthropometry specifications by Reed et al. [9]. Mass and stature of 48.2 kg and 1.508 meters defined by Schneider et al. [10], same as the THOR-5F design [11], were used as the input to generate the neck anthropometry specifications. The cord length between the occipital condyle (OC) joint and the C7/T1 from the University of Michigan Transportation Institute (UMTRI) Anthropometry for Motor Vehicle Occupant (AMVO) 5th percentile female (5F) was used to control the overall neck length when generating the female neck anthropometry. The nodes from the anthropometry model generated for the THOR-AV 5F neck are shown in Fig. 1.

The neck design of the THOR-AV 5F is shown in Fig. 2. Applying the same concept as the THOR-AV 50M neck design, the upper neck load cell was packaged into the head to make room for a torsion element. A representative neck curvature and an increased cross-section were incorporated into the neck design to represent the 5th percentile female neck more accurately. The joint at the bottom of the neck has an increased range of motion for the head angle adjustment. The dummy cross-sectional area was determined by finite element modeling, focusing on kinematics and neck bending curvature. The analysis indicated a gradual increment of the cross-sectional area from C1 to C7 would provide closer human-like bending curvature.

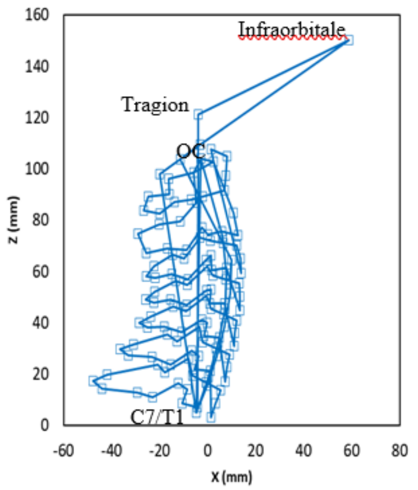

Fig. 1. Neck model generated from the parametric model defined by Reed et al.[9]

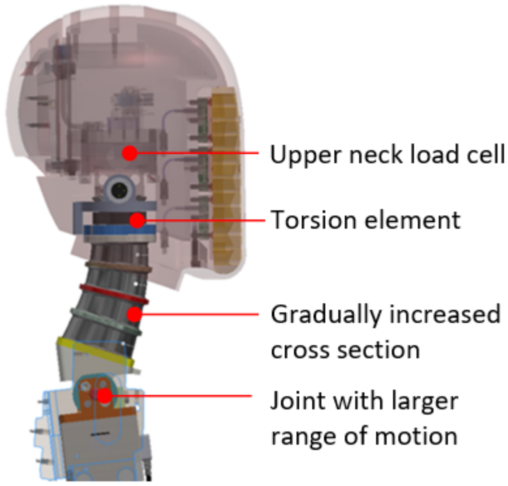

Fig. 2. THOR 5F neck design

The aim of this study is to evaluate the biofidelity of the THOR-AV 5F neck and conduct a preliminary evaluation of the neck repeatability and reproducibility.

II. METHODS

The test method and equipment used in this study were the same as the ones documented in Wang et al.[6] for the 50th percentile male neck. The same sled pulse for each test condition was used as well accordingly. The frontal, lateral, and oblique impact tests were conducted on a mini-sled named E-Liner Dummy Cert Sled (Humanetics, Farmington Hills, Michigan, USA), which is a programable magnetic sled. The sled can generate an input pulse precisely in accordance with the pre-programmed acceleration. The neck torsion evaluation was conducted with the PMHS test rig at the Injury Biomechanics Research Center (IBRC) of The Ohio State University.

PMHS Corridor Scaling

Since there is no PMHS test data available for the 5th female, a scaling method used by Lee et al. [12] was used to derive the 5th percentile female corridors from the 50th percentile male biofidelity corridors. Since Lee et al. [12] already provided the scaled 5th percentile female corridors for the frontal flexion and lateral flexion from

Thunnissen et el. [3] and Wismans et al. [4], respectively, these two sets of corridors were used in this study without any change. The 50th percentile male PMHS corridors published by Kang et al. [6] were scaled in accordance with the same method described in Lee et al. [12]. The scaling factors are summarized in TABLE I.

TABLE I
SUMMARY OF THE SCALING FACTORS DEFINED IN LEE ET AL. [12]

Description	*Symbol*	*Scale factors*
Mass	λm	0.60
Dimension	λx, λy	0.81
	λz	0.91
Moment	λ_M	0.53
Head/neck angle	$\lambda\theta$	1.12
Neck bending stiffness	λk	0.57
Head CG displacement	$\lambda\delta x$	1.02
	$\lambda\delta z$	0.91
Head Acceleration	λa	0.98
Head Acceleration Time	λt	1.02
Neck Torsion Moment	λ_T	0.53
Neck Torsion Angle	$\lambda\psi$	1.12

It was noticed that the corridors of head y-rotation and head z-displacement in the Thunnissen et al. frontal test condition started approximately 20 ms later than sled acceleration and other corridors. A correction was made to these two corridors so that they are synchronized with the sled pulse and other corridors. It is worth noting that this shift does not affect the BioRank scores (B) with the NHTSA BioRank method used in this study. However, it does influence the dummy phase shift time (DPS), which is for monitoring purposes only [14][15]. For the neck torsion test, there was only one PMHS test. This test was treated as the mean of the corridor. The upper and lower corridors were created with plus and minus 20% of the test data, respectively.

Test Matrix

Three necks were fabricated from the same mold for evaluation in this study. The necks were made of Butyl rubber. The stiffness of the rubber was adjusted to optimize the biofidelity responses, and the results shown in this paper were the final design. The necks were manually assembled and placed in the laboratory environment (20.6 - 22.2°C deg, 10-70% humidity) for 4 hours before any test was conducted. Each neck was tested three times in each test condition. Since good repeatability was observed in frontal, lateral, and oblique tests, only one neck was selected for evaluation in the torsion test condition. The tests conducted in this study are summarized in TABLE II.

TABLE II
TEST MATRIX

Test Condition	Reference	Neck Serial No.
Frontal	Thunnissen et al. 1993	EW2277, EW2279, EW2282
	Kang et al. 2018	EW2277, EW2279, EW2282
Lateral	Wismans et al. 1983	EW2277, EW2279, EW2282
	Kang et al. 2018	EW2277, EW2279, EW2282
Oblique	Kang et al. 2018	EW2277, EW2279, EW2282
Torsion	Kang et al. 2018	EW2282

Data Processing

The instrumentation complies with SAE J211 requirements. The data were filtered with the same filter as their corresponding PMHS test.

BioRank Method

NHTSA BioRank method was used to calculate the BioRank scores (BRS, also abbreviated as B in the tables) to assess biofidelity. The fundamental calculation method was defined by Rhule et al. [13], and refined later by Kang et al. and Hagedorn et al. [14][15]. The data were filtered before the BioRank score calculation. The dummy data were aligned with the biofidelity corridor mean by one of the following three methods: 1) the lowest Dummy Cumulative Absolute Difference (DCAD), or 2) the first peak, or 3) no shift at all. The best alignment was selected for the BioRank score calculation. The BioRank score (B) was defined as DCAD/CCSD (cadaver cumulative standard deviation). The dummy phase shift (DPS), the time shift of the dummy data curve for DCAD calculation, was recorded for monitoring. The correlation between the dummy biofidelity and its BioRank scores are defined in TABLE III [16]. Further information on the most updated NHTSA BioRank method can be found in Hagedorn et al. [15].

TABLE III
CORRELATION BETWEEN BIOFIDELITY AND THE BIORANK SCORES

BioRank Score	B ≤ 1.0	1.0 < B ≤ 2.0	2.0 < B ≤ 3.0	B > 3.0
Biofidelity	Excellent	Good	Marginal	Poor

The BioRank score for each test was calculated and averaged to calculate the score for the neck, with one exception of the torsion test (N=1). The final BioRank score was calculated by averaging the BioRank scores of all three necks.

III. RESULTS

The BioRank scores are summarized in this section, and the time history plots of the data without phase shift are attached in the Appendix.

Frontal Impact

The BRS scores of the neck in the Thunnissen et al. frontal impact test condition are summarized in TABLE IV. The overall BRS score for this test condition is 1.26, corresponding to *good* biofidelity. The BRS scores of head resultant acceleration, head y-rotation, head CG x-displacement, and head z-displacement are 1.49, 0.84, 1.10 and 0.72, corresponding to *good*, *excellent*, *good,* and *excellent* biofidelity, respectively. The neck linkage (T1-OC) rotation has a BRS score of 2.17, corresponding to *marginal* biofidelity.

TABLE IV
BRS SCORES OF THOR-AV 5F NECK IN THUNNISSEN ET AL. FRONTAL IMPACT TEST CONDITION

	Head Res. Accel		Head Rot. Y		Neck Rot. Y		Head CG Displ. X		Head CG Displ. Z		Average
Test ID	B	DPS (ms)	B	DPS (ms)	B	DPS (ms)	B	DPS (ms)	B	DPS (ms)	
EW2277-3	1.57	-1	0.94	-3	2.08	-6	0.99	-1	0.87	1	
EW2277-4	1.40	0	0.88	-1	1.80	-3	1.03	0	0.87	3	
EW2277-5	1.41	0	0.89	-2	1.78	-4	0.88	1	0.95	3	
Average	**1.46**	0	**0.90**	-2	**1.89**	-4	**0.96**	0	**0.90**	2	**1.22**
EW2279-1	1.65	2	0.74	1	2.62	-4	1.42	2	0.54	6	
EW2279-2	1.49	1	0.80	-2	2.23	-9	1.05	-1	0.65	0	
EW2279-3	1.36	1	0.82	-5	2.08	-10	0.97	-5	0.69	-5	
Average	**1.50**	1	**0.79**	-2	**2.31**	-8	**1.15**	-1	**0.63**	1	**1.27**
EW2282-1	1.58	2	0.75	-5	2.48	-7	1.47	-3	0.56	0	
EW2282-2	1.47	2	0.87	4	2.16	-1	1.11	5	0.64	7	
EW2282-3	1.47	1	0.88	0	2.28	-6	1.00	1	0.74	2	
Average	**1.51**	1	**0.84**	0	**2.30**	-5	**1.19**	1	**0.65**	3	**1.30**
Overall	**1.49**	1	**0.84**	-2	**2.17**	-5	**1.10**	0	**0.72**	2	**1.26**

The BRS scores of the neck in Kang et al. frontal impact test condition are summarized in TABLE V. The overall BRS score is 1.60 for this test, corresponding to *good* biofidelity. Except for the lower neck y-moment, the BRS scores of all evaluated parameters are between 1.0 and 2.0, corresponding to *good* biofidelity. It was observed that the lower neck y-moment has an average BRS score of 2.77 for the three necks evaluated, corresponding to *marginal* biofidelity. The y-moment of the dummy had a higher first peak and dropped quicker than the PMHS responses, shown in Fig. A12.

TABLE V
BRS SCORES OF THE NECK IN FRONTAL KANG ET AL. FRONTAL IMPACT TEST CONDITION

	Head Ax		Head Az		Head Rot Y		Neck Fx		Neck Fz		Neck My		
Test ID	B	DPS (ms)	B	DPS (ms)	B	DPS (ms)	B	DPS (ms)	B	DPS (ms)	B	DPS (ms)	Avg
EW2277-1	1.24	22	1.00	12	1.30	58	1.69	-92	1.36	32	2.68	36	
EW2277-2	1.26	21	0.98	12	1.37	64	1.47	-92	1.38	32	2.68	36	
EW2277-3	1.26	21	0.98	13	1.37	61	1.66	-92	1.37	32	2.68	36	
Average	**1.25**	21	**0.99**	12	**1.35**	61	**1.61**	-92	**1.37**	32	**2.68**	36	**1.54**
EW2279-1	1.38	26	1.03	11	1.52	80	1.79	-87	1.42	33	2.88	39	
EW2279-2	1.35	23	1.08	12	1.43	64	1.73	-88	1.40	32	2.83	38	
EW2279-3	1.34	25	1.03	13	1.45	58	1.77	-92	1.41	33	2.83	38	
Average	**1.35**	25	**1.05**	12	**1.47**	67	**1.76**	-89	**1.41**	33	**2.84**	38	**1.65**
EW2282-1	1.32	25	1.05	14	1.44	64	1.74	-89	1.43	32	2.80	38	
EW2282-2	1.31	23	1.02	12	1.41	66	1.78	-92	1.41	32	2.78	37	
EW2282-3	1.31	23	1.04	13	1.40	66	1.73	-92	1.40	32	2.78	37	
Average	**1.31**	23	**1.03**	13	**1.41**	65	**1.75**	-91	**1.41**	32	**2.79**	37	**1.62**
Overall	**1.31**	23	**1.02**	13	**1.41**	64	**1.71**	-91	**1.40**	32	**2.77**	37	**1.60**

Lateral Impact

The BRS scores of the neck in Wismans et al. [4] lateral impact test condition are summarized in TABLE VI. It was observed that the magnitudes of the head CG y- and z-displacement are less than the PMHS responses, shown in Fig. A16 and Fig. A17 in the Appendix, respectively. The BRS scores for x-, y- and z-displacement are 2.13, 3.60 and 1.43, corresponding to *marginal*, *poor,* and *good* biofidelity, respectively.

TABLE VI
BRS SCORES OF THE NECK IN WISMANS ET AL. LATERAL IMPACT TEST CONDITION

	Head rotation X		Head CG Displ. Y		Head CG Displ. Z		
TestID	B	DPS(ms)	B	DPS(ms)	B	DPS(ms)	Average
EW2277-1	2.19	7	3.89	-3	1.72	7	
EW2277-2	2.00	7	3.48	-3	1.35	3	
EW2277-3	1.89	7	3.50	-3	1.39	6	
Average	**2.03**	7	**3.62**	-3	**1.49**	5	**2.38**
EW2279-1	2.39	9	3.95	-1	1.67	4	
EW2279-2	2.16	11	3.60	0	1.41	8	
EW2279-3	2.05	6	3.59	-5	1.35	1	
Average	**2.20**	8	**3.71**	-2	**1.48**	4	**2.46**
EW2282-1	2.29	13	3.62	3	1.46	7	
EW2282-2	2.09	12	3.34	2	1.20	9	
EW2282-3	2.11	4	3.45	-7	1.30	1	
Average	**2.16**	9	**3.47**	-1	**1.32**	6	**2.32**
Overall	**2.13**	8	**3.60**	-2	**1.43**	5	**2.39**

The BRS scores of the neck in Kang et al. lateral impact test condition are summarized in TABLE VII. The overall BRS score is 1.65, corresponding to *good* biofidelity. The head y- and z-acceleration, lower neck z-force, and x-moment demonstrated good biofidelity with BRS scores of 1.11, 1.40, 1.33, and 1.95, respectively. The head x-rotation demonstrated *excellent* biofidelity with a BRS score of 0.37, while the lower neck y-force showed *poor* biofidelity with a BRS score of 3.76.

TABLE VII
BRS SCORES OF THE NECK IN KANG ET AL. LATERAL IMPACT TEST CONDITION

	Head Ay		Head Az		Head Rot. X		Lower Neck Fy		Lower Neck Fz		Lower Neck Mx		
Test ID	B	DPS (ms)	B	DPS (ms)	B	DPS (ms)	B	DPS (ms)	B	DPS (ms)	B	DPS (ms)	Avg.
EW2277-1	1.10	35	1.39	9	0.38	19	3.71	-73	1.30	21	1.94	17	
EW2277-2	1.06	33	1.36	10	0.35	19	3.72	-73	1.33	20	1.91	17	
EW2277-3	1.07	33	1.35	9	0.34	21	3.73	-73	1.34	20	1.91	16	
Average	**1.08**	34	**1.36**	9	**0.36**	20	**3.72**	-73	**1.32**	20	**1.92**	17	**1.63**
EW2279-1	1.14	34	1.47	8	0.41	26	3.76	-73	1.30	22	2.03	18	
EW2279-2	1.13	34	1.40	9	0.38	27	3.80	-73	1.37	22	2.01	17	
EW2279-3	1.15	35	1.40	9	0.37	25	3.82	-73	1.29	21	1.99	17	
Average	**1.14**	34	**1.42**	9	**0.38**	26	**3.79**	-73	**1.32**	22	**2.01**	17	**1.68**
EW2282-1	1.11	34	1.40	9	0.37	22	3.74	-73	1.34	21	1.93	17	
EW2282-2	1.09	33	1.39	10	0.36	25	3.77	-73	1.38	20	1.93	16	
EW2282-3	1.15	34	1.41	9	0.35	17	3.76	-73	1.30	21	1.93	16	
Average	**1.12**	34	**1.40**	9	**0.36**	22	**3.75**	-73	**1.34**	21	**1.93**	16	**1.65**
Overall	**1.11**	34	**1.40**	9	**0.37**	22	**3.76**	-73	**1.33**	21	**1.95**	17	**1.65**

Oblique Impact

The BRS scores of the neck in Kang et al. oblique test condition are summarized in TABLE VIII. The overall BRS score for this test condition is 2.77, corresponding to *marginal* biofidelity. The head x-rotation has a BRS score of 0.50, corresponding to excellent biofidelity. The head y- and z-acceleration, head z-rotation, lower neck z-force, and x-moment have BRS scores of 1.62, 1.22, 1.35, 1.52, and 1.38, respectively, all corresponding to *good* biofidelity. The head x-acceleration and lower neck x-force have BRS scores of 2.71 and 2.59, respectively, both corresponding to *marginal* biofidelity. The head y-rotation, lower neck y-force, y-moment, and z-moment have BRS scores greater than 3.0, corresponding to *poor* biofidelity.

TABLE VIII
BRS SCORES OF THE NECK IN KANG ET AL. OBLIQUE IMPACT TEST CONDITION

	Head Ax		Head Ay		Head Az		Head Rot X		Head Rot. Y		Head Rot. Z	
Test ID	B	DPS (ms)	B	DPS (ms)	B	DPS (ms)	B	DPS (ms)	B	DPS (ms)	B	DPS (ms)
EW2277-1	2.73	27	1.61	41	1.31	5	0.50	11	3.12	56	1.36	73
EW2277-2	2.68	24	1.61	39	1.23	5	0.48	10	2.72	52	1.36	73
EW2277-3	2.67	23	1.59	38	1.23	6	0.50	9	2.95	54	1.33	73
Average	**2.69**	25	**1.60**	39	**1.26**	5	**0.50**	10	**2.93**	54	**1.35**	73
EW2279-1	2.73	26	1.64	40	1.27	7	0.51	11	3.32	60	1.30	73
EW2279-2	2.70	24	1.59	39	1.22	5	0.47	11	2.87	55	1.28	73
EW2279-3	2.70	24	1.60	38	1.18	6	0.48	10	3.01	56	1.36	73
Average	**2.71**	25	**1.61**	39	**1.23**	6	**0.48**	11	**3.07**	57	**1.31**	73
EW2282-1	2.72	23	1.62	38	1.20	5	0.49	9	3.29	56	1.43	73
EW2282-2	2.73	23	1.70	39	1.18	4	0.53	9	3.69	58	1.40	73
EW2282-3	2.72	24	1.63	39	1.16	5	0.49	9	2.57	53	1.36	73
Average	**2.72**	24	**1.65**	39	**1.18**	5	**0.51**	9	**3.18**	56	**1.40**	73
Overall	**2.71**	24	**1.62**	39	**1.22**	5	**0.50**	10	**3.06**	55	**1.35**	73

TABLE VIII (CONTINUED)
BRS SCORES OF THE NECK IN KANG ET AL. OBLIQUE IMPACT TEST CONDITION

	Lower Neck Fx		Lower Neck Fy		Lower Neck Fz		Lower Neck Mx		Lower Neck My		Lower Neck Mz		
Test ID	B	DPS (ms)	B	DPS (ms)	B	DPS (ms)	B	DPS (ms)	B	DPS (ms)	B	DPS (ms)	Avg.
EW2277-1	2.45	-71	3.46	-73	1.54	26	1.42	33	10.80	36	3.26	38	
EW2277-2	2.58	-70	3.47	-73	1.51	26	1.38	32	10.44	33	3.25	37	
EW2277-3	2.47	-73	3.45	-73	1.52	25	1.36	32	10.35	33	3.20	37	
Average	**2.50**	-72	**3.46**	-73	**1.52**	26	**1.38**	32	**10.53**	34	**3.24**	37	**2.75**
EW2279-1	2.73	-70	3.53	-73	1.55	27	1.43	33	11.15	38	3.26	36	
EW2279-2	2.61	-70	3.52	-73	1.54	26	1.40	32	10.82	35	3.22	36	
EW2279-3	2.66	-71	3.49	-73	1.51	25	1.39	31	10.69	34	3.19	36	
Average	**2.67**	-70	**3.51**	-73	**1.53**	26	**1.41**	32	**10.89**	36	**3.23**	36	**2.80**
EW2282-1	2.58	-70	3.41	-73	1.51	25	1.35	31	10.46	33	2.97	33	
EW2282-2	2.59	-71	3.44	-73	1.52	24	1.35	31	10.45	33	2.99	33	
EW2282-3	2.66	-71	3.43	-73	1.50	25	1.35	31	10.41	33	3.03	33	
Average	**2.61**	-70	**3.43**	-73	**1.51**	24	**1.35**	31	**10.44**	33	**3.00**	33	**2.75**
Overall	**2.59**	-71	**3.46**	-73	**1.52**	25	**1.38**	32	**10.62**	34	**3.15**	35	**2.77**

Torsion Impact

The BRS scores of the neck in Kang et al. torsion impact test along the z-axis are summarized in TABLE IX. The overall BRS score of the neck in this test condition is 2.08, corresponding to *marginal* biofidelity. The z-rotation and lower neck z-moment have BRS scores of 1.47 and 2.69, corresponding to *good* and *marginal* biofidelity, respectively.

TABLE IX
BRS SCORES OF THE NECK IN KANG ET AL. TORSION TEST CONDITION

	Rotation Z		Lower Neck Mz		Average
Test ID	B-Rz	DPS-Rz	B-Mz	DPS-Mz	
EW2282-1	1.29	0	1.92	0	
EW2282-2	1.57	0	2.75	0	
EW2282-3	1.55	0	3.39	0	
Average	1.47	0	2.69	0.00	2.08

Overall Biofidelity

The overall BRS scores are summarized in TABLE X. In the frontal impact test conditions, the overall BRS scores for both Thunnissen et al. and Kang et al. test conditions are 1.26 and 1.60, respectively, both corresponding to *good* biofidelity. In lateral test conditions, the BRS scores for Wismans et al. and Kang et al. test conditions are 2.39 and 1.65, corresponding to *marginal* and *good* biofidelity, respectively. The BRS scores for both oblique and torsion in Kang et al. test conditions are 2.08, corresponding to marginal biofidelity. Overall, the neck biofidelity has a BRS score of 1.96, corresponding to good biofidelity.

TABLE X
SUMMARY OF THE OVERALL BRS SCORES

	Neck SN	EW2277	EW2279	EW2282	Average
Frontal	Thunnissen et al.	1.22	1.27	1.30	1.26
	Kang et al.	1.54	1.65	1.62	1.60
Lateral	Wismans et al.	2.38	2.46	2.32	2.39
	Kang et al.	1.63	1.68	1.65	1.65
Oblique	Kang et al.	2.75	2.80	2.75	2.77
Torsion	Kang et al.	NA	NA	2.08	2.08
Overall					1.96

DISCUSSION

From the summary of the BRS scores summarized in TABLE X, it was observed there is a large difference in BRS scores between Wismans et al. and Kang et al. test conditions. A similar pattern was observed in the THOR-AV 50M neck [6]. The lateral biofidelity corridor developed by Wismans et al. [4] was based on film data from the Naval Biodynamic Laboratory (NBDL) volunteer tests that were conducted in the 1970s. The accuracy of the measurements in NBDL tests might not be as accurate as the research conducted in Kang et al. [6] in 2018. In addition, NDBL data only had head y-rotation, head x and z-displacement available, missing head accelerations and lower neck forces and moment, which were provided in Kang et al. For these reasons, Wismans et al. may not have enough data to provide a comprehensive BioRank evaluation for lateral impact.

In the Kang et al. torsion test, it was noticed that the THOR-AV 5F neck torsion element provided a higher neck z-moment than the PMHS responses, shown in Fig. 3. As mentioned earlier in this paper, there was only one PMHS test data available, which is not sufficient to create a statistically meaningful corridor. The torsion biofidelity corridor was generated by using the sole PMHS test data as its mean, which may not reflect the mean value if there were more PMHS test data available. In addition, the scaling method could be another source of corridor inaccuracy.

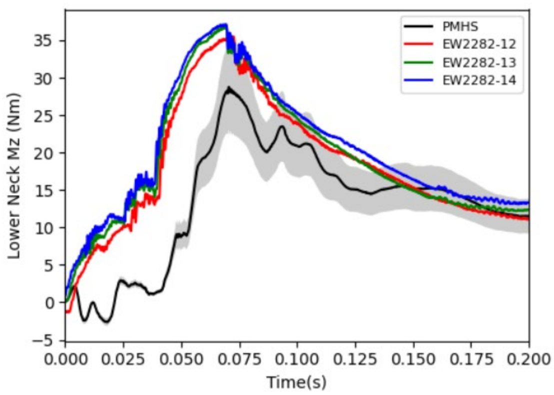

Fig. 3. Lower neck moment in Kang et al. torsion test condition.

It was observed that a few data channels, for example, the head x-rotation in the lateral Kang test condition, shown in Fig. 4, have a BRS score of 0.37, which was caused by a wide corridor width. The low BRS score of 0.37 indicated excellent biofidelity. However, the peak magnitude is only approximately half of the PMHS corridor mean value, indicating *marginal or poor* biofidelity from engineering judgment. It was also observed that a narrow biofidelity corridor would make it extremely challenging to achieve a good biofidelity. Even a good match between ATD and PMHS responses can still yield a high BRS score due to a narrow corridor width. In ATD development, the PMHS mean was always targeted for ATD biofidelity responses. To address these extreme conditions, a mean plus/minus a percentage of the mean value would provide better guidance for dummy development. Other methods, such as a uniform corridor width could be considered as well, knowing these may not be a perfect but reasonable option to address the situation.

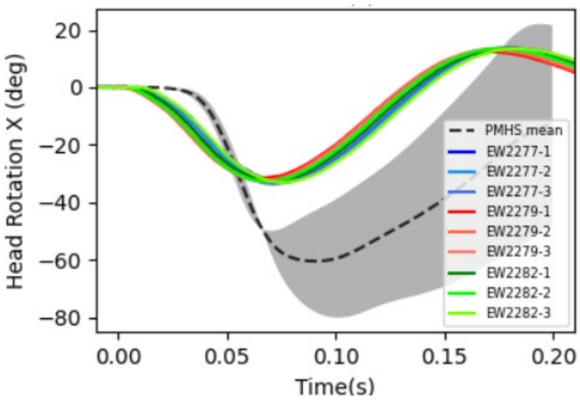

Fig. 4. Head x-rotation in Kang et al. lateral test condition

The biofidelity corridors were scaled from 50th percentile male corridors. The scaling method used a very simple model to represent a complex human body structure, which could lead to inaccurate corridors. Testing of 5th percentile female PMHS is desired to develop more accurate biofidelity corridors for ATD neck development.

IV. CONCLUSIONS

THOR-AV 5F neck was developed based on the same concept used in THOR-AV 50M design. The biofidelity of the neck showed very promising results with future improvements in torsion response desired. The THOR-AV 5F neck has BRS scores of 1.26 and 1.60 in both frontal test conditions, corresponding to *good* biofidelity. The THOR-AV 5F neck has a BRS score of 2.39 and 1.65 in Wismans et al. and Kang et al. lateral test conditions, corresponding to *marginal* and *good* biofidelity. We believe the biofidelity in Kang et al. lateral test condition is more accurate and representative of the neck responses. The THOR-AV 5F neck has BRS scores of 2.77 and 2.08 in oblique and torsion conditions, respectively, corresponding to *marginal* biofidelity. The neck has an overall biofidelity score of 1.96, corresponding to *good* biofidelity.

V. LIMITATIONS AND FUTURE WORK

There were limited PMHS tests in Kang et al. [6], i.e., frontal (N=3), lateral (N=3), oblique (N=2) and torsion (N=1). Additional PMHS tests would offer more accurate biofidelity guidance for ATD design, especially the torsion test. Furthermore, the scaling method was based on simple engineering mechanics theory and would introduce inaccuracy to the scaled corridors. To address these concerns, fifth percentile PMHS tests are desired.

In the future, the authors plan to evaluate the Hybrid III and THOR 5th female necks for comparison. THOR-AV 5F neck torsion element material will also be explored for potential improvement of its biofidelity.

VI. ACKNOWLEDGMENT

The tests were conducted in the ATD test lab of Humanetics Innovative Solutions, Inc. and the Injury Biomechanics Research Center of The Ohio State University. The views expressed are these of the authors and may not represent the views of their respective organizations.

VII. REFERENCES

[1] Foster J.K., Kortge, J.O., and Wolanin M.J., Hybrid III – a biomechanically-based crash test dummy, SAE Transactions, Vol. 86, section 4, 770720-771010(1977), pp. 3268-3383. https://www.jstor.org/stable/44644622.

[2] Mertz, H. and Patrick, L., "Strength and Response of the Human Neck*," SAE Technical Paper 710855, Fifteenth Stapp Cra Crash Conference, 1971, https://doi.org/10.4271/710855.

[3] Thunnissen J., Wismans, J. Ewing C.L., Thomas D.J., 1995. Human Volunteer Head-Neck Response in Frontal Flexion: A New Analysis. Thirty-ninth Stapp Car Crash Conference, San Diego, California, November 8-10, SAE Paper # 952721.

[4] Wismans J. and Spenny C.H., 1983, Performance requirements for mechanical necks in lateral flexion, Proceedings of 27th Stapp Car Crash Conference, SAE paper No. 831613, Warrendale, PA 15096, pp137-148.

[5] Wang, Z.J., Lee, E., Bolte IV, J., Below, J., Loeber, B., Ramachandra, R., Greenless, B., Guck, D., Biofidelity evaluation of THOR 5th percentile female ATD, Proceedings of IRCOBI Conference, 2018.

[6] Wang, Z.J., Loeber, B., Tesny, A., Hu, G., Kang, Y.S., Neck biofidelity of THOR-AV, THOR and Hybrid III 50th dummies. *Proceedings of IRCOBI Conference*, 2021, virtual.
[7] Kang Y-S., Stammen J., Moorhouse K., Bolte J., Head and neck responses of post-mortem subjects in frontal, oblique, side and twist scenarios. 2018 International Research Council on the Biomechanics of Injury (IRCOBI) Conference Proceedings, 12 – 14 September 2018 – Athens, Greece.
[8] Wang, Z., McInnis, J., Benfant, L. Feng, Z., Lee, E., THOR 5th percentile female ATD design. Proceedings of the 25th International Technical Conference on the Enhanced Safety of Vehicles (ESV) Detroit, Michigan USA, June 2017.
[9] Reed, M.P., Jones, M.L.H., A parametric model of cervical spine geometry and posture. The University of Michigan Deep Blue Documents, Report UMTRI-2017-1, https://deepblue.lib.umich.edu/handle/2027.42/137652.
[10] Schneider, L.W., Robbins, D.H., Pflug, M.A., Snyder, R.G., 1983. Anthropometry Specifications for Small Female & Large Male Dummies, Vol. 3, UMTRI-83-53-3.
[11] Wang, Z., Lee, E., McInnis, J., Benfant, L., Feng, Z. 25th ESV Conference Proceedings, June 5-8, 2017. Detroit, Michigan, USA.
[12] Lee, E.L., Parent, D.P., McFadden, M.J. and Moorhouse K., 2017. Biomechanical response requirements Manual: THOR 5th percentile female NTHSA advanced frontal dummy. NHTSA report #: DOT HS 812 370.
[13] Rhule, H., Sticklin, J., Donnelly, B., Moorhouse, K., 2018. Improvements to NHTSA's Biofidelity Ranking System and Application to the Evaluation of the THOR 5th Female Dummy, 2018 IRCOBI Conference Proceedings, September 12 -14, 2018, Athens, Greece.
[14] Kang Y-S, Stammen J., Ramachandra R., Agnew A.M., Hagedorn A., Thomas C., Kwon H.J., Moorhouse K., Bolte IV J.H., 2020. Biomechanical responses and injury assessment of post mortem human subjects in various rear-facing configurations. Stapp Car Crash Journal, Vol 64, pp 155-212.
[15] Hagedorn A., et al. Biofidelity evaluation of THOR-50M in rear-facing seating configurations using an updated BioRank system, SAE International Journal of Transportation Safety (February 2022), Special Issue: Occupant Protection & Crashworthiness for ADS-Equipped Vehicles.

VIII. APPENDIX

The plots of all tests are listed in this appendix.

Frontal impact – Thunnissen et al.[3]

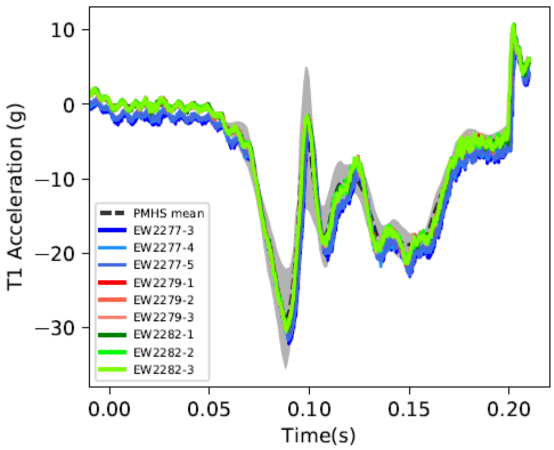

Fig. A1. T1 (mini-sled) acceleration

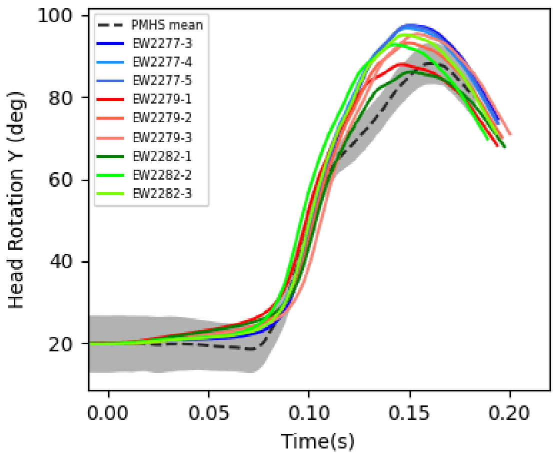

Fig. A2. Head rotation Y

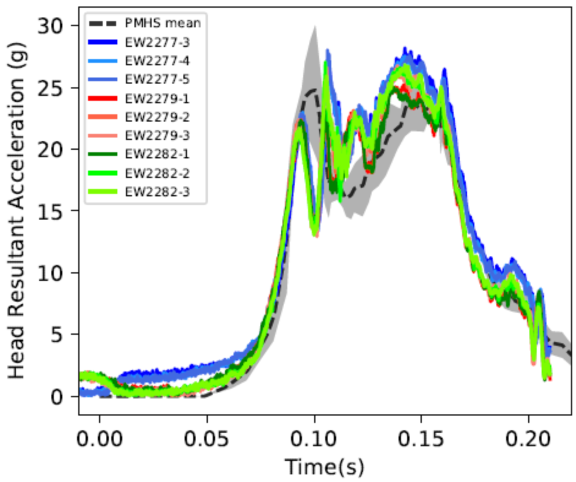

Fig. A3. Head resultant acceleration

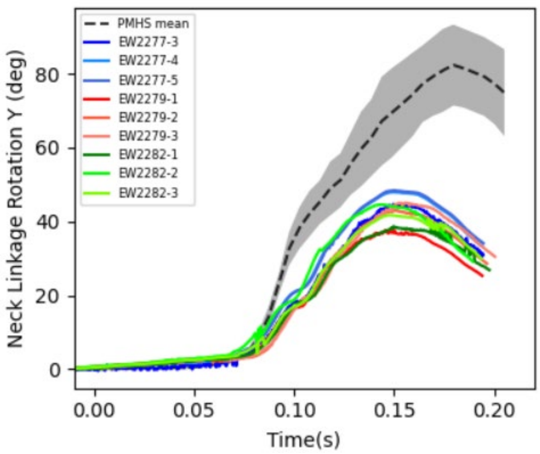

Fig. A4. Neck rotation Y

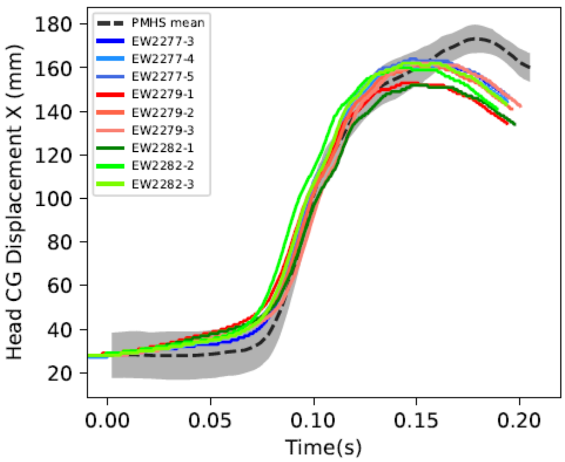

Fig. A5 Head CG displacement X

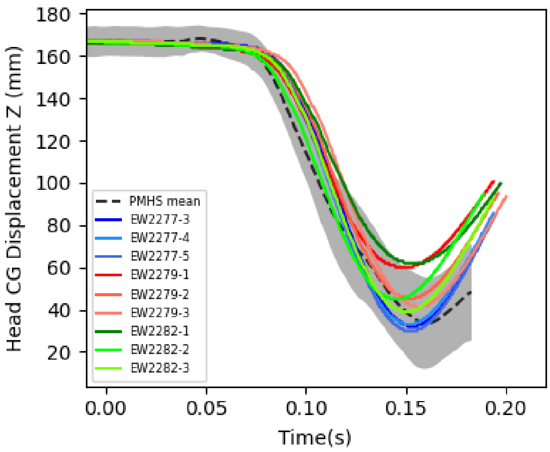

Fig. A6 Head CG displacement Z

Frontal impact – Kang et al. *[6]*

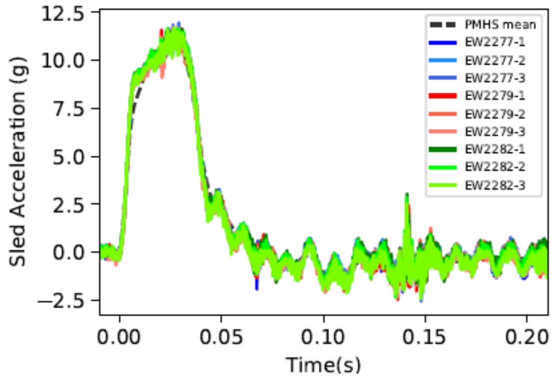

Fig. A7. Sled acceleration

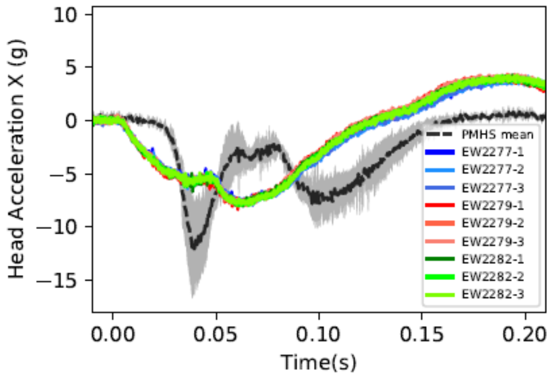

Fig. A8 Head acceleration X

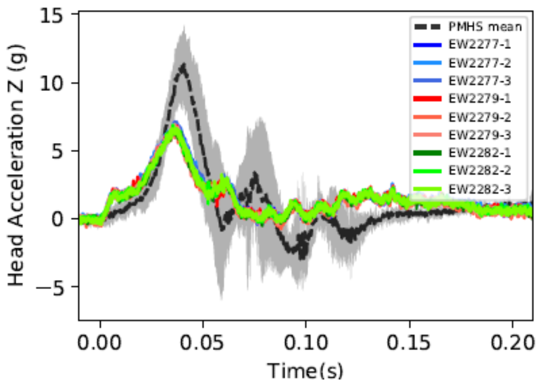

Fig. A9. Head acceleration Z

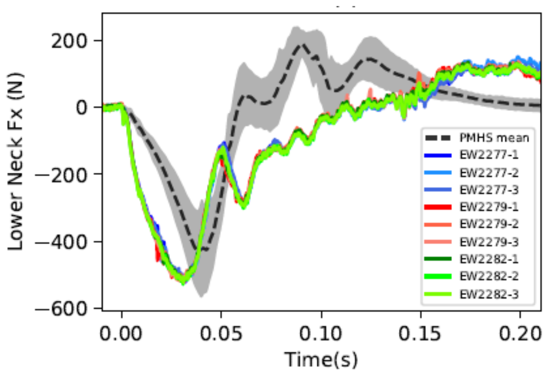

Fig. A10. Lower neck force X

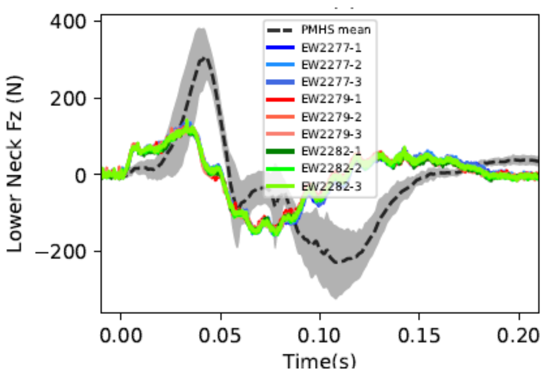

Fig. A11. Lower neck force Z

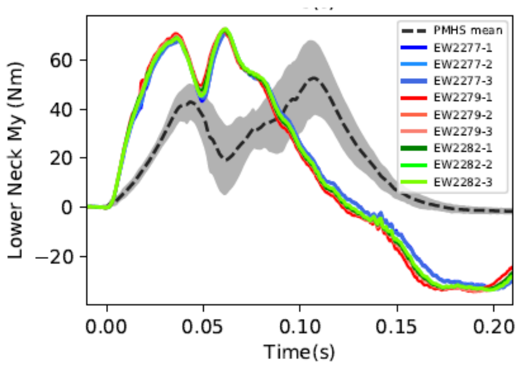

Fig. A12. Lower neck moment Y

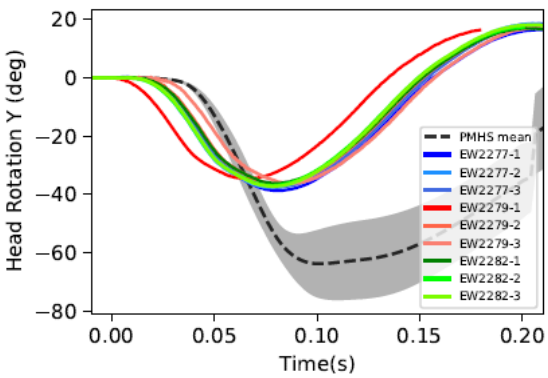

Fig. A 13. Head rotation Y

Lateral Impact – Wismans et al. [4]

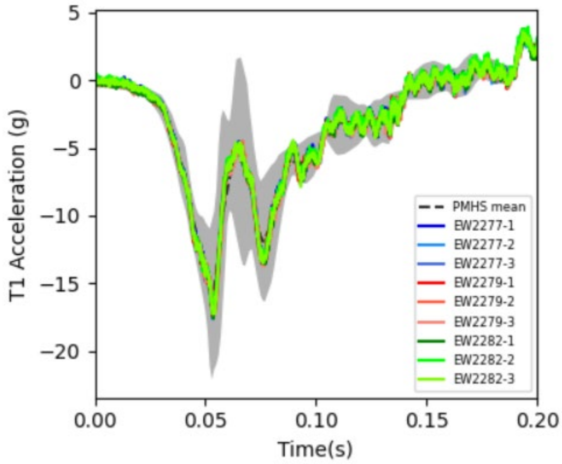

Fig. A14. T1 acceleration (mini-sled pulse)

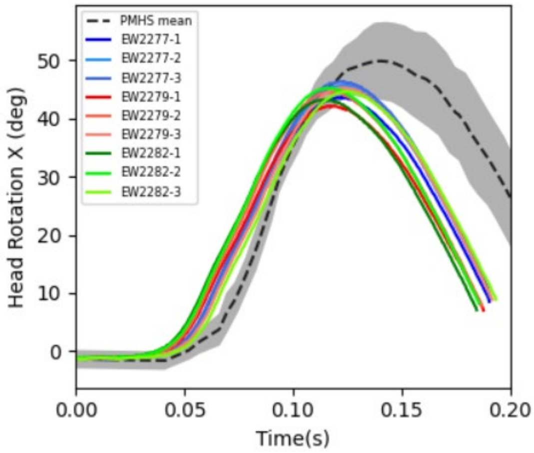

Fig. A 15. Head rotation in x-axis

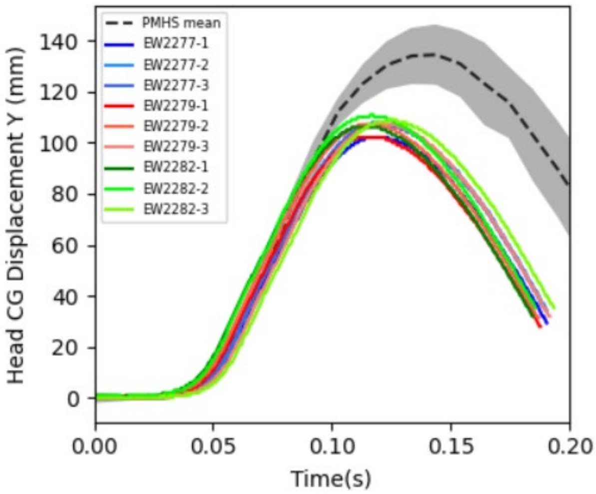

Fig. A16. Head CG y-displacement

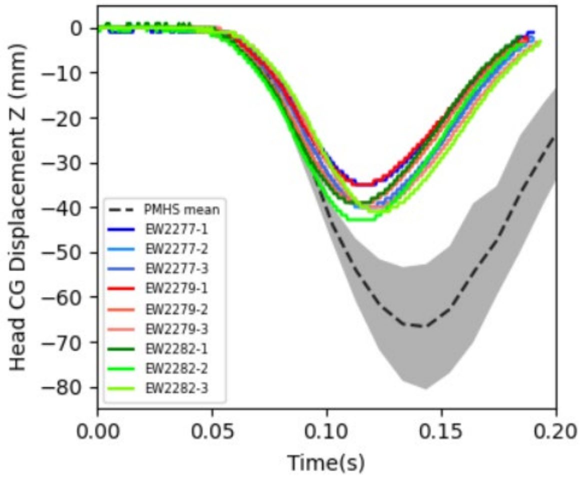

Fig. A17. Head CG z-displacement

Lateral Impact – Kang et al. [6]

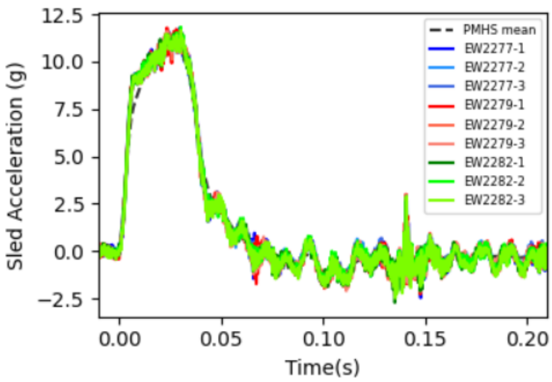

Fig. A18. Sled acceleration

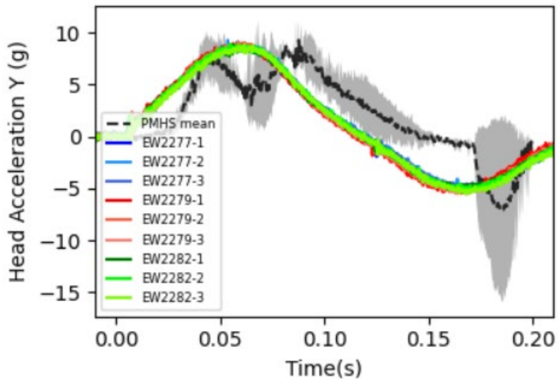

Fig. A19. Head acceleration Y

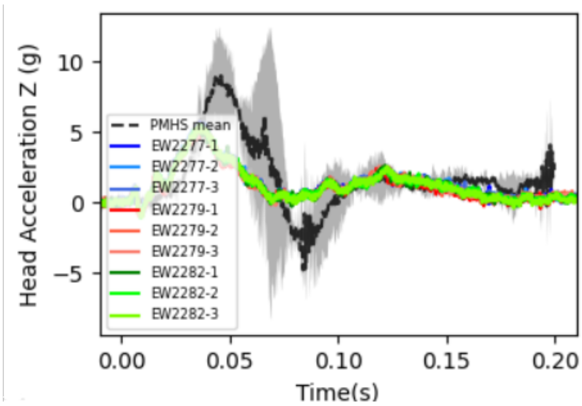

Fig. A20. Head acceleration Z

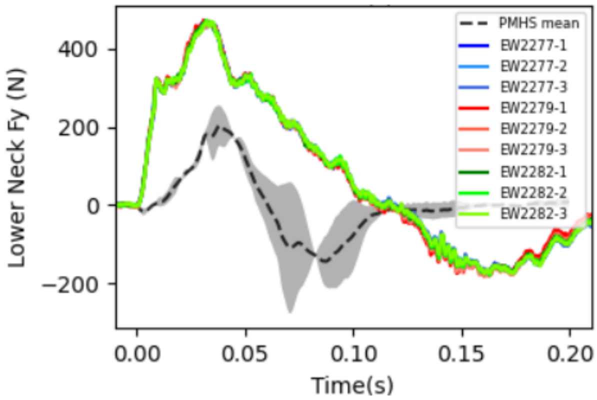

Fig. A21. Lower Neck Force Y

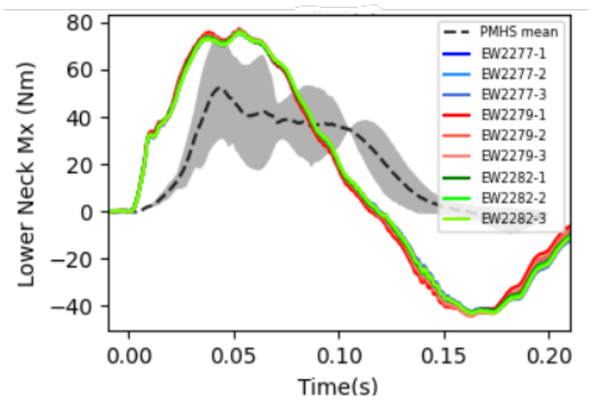

Fig. A22. Lower neck moment X

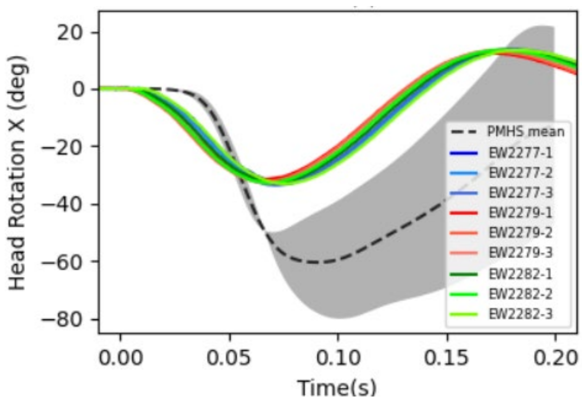

Fig. A23 Head rotation X

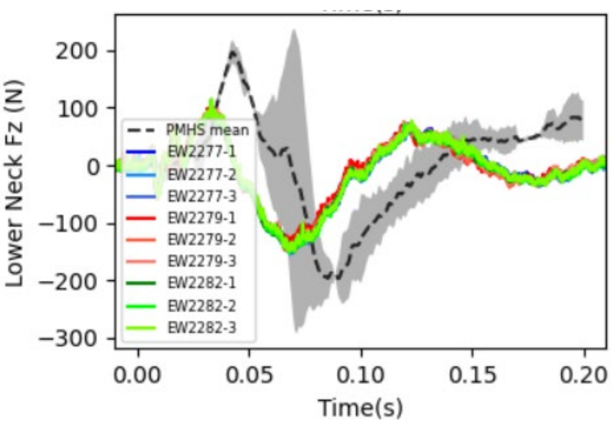

Fig. A24. Lower neck force Z

Oblique Impact – Kang et al. [6]

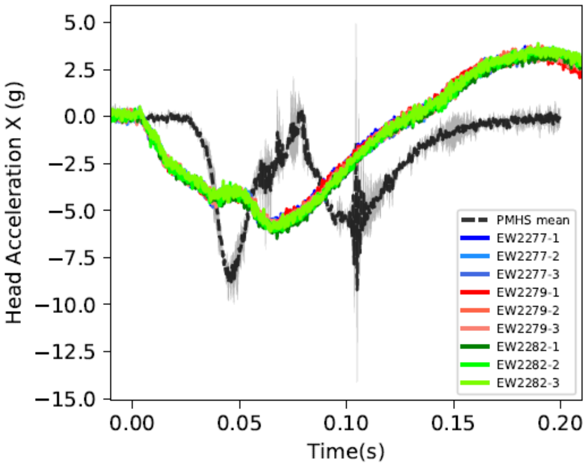

Fig. A25. Head acceleration X

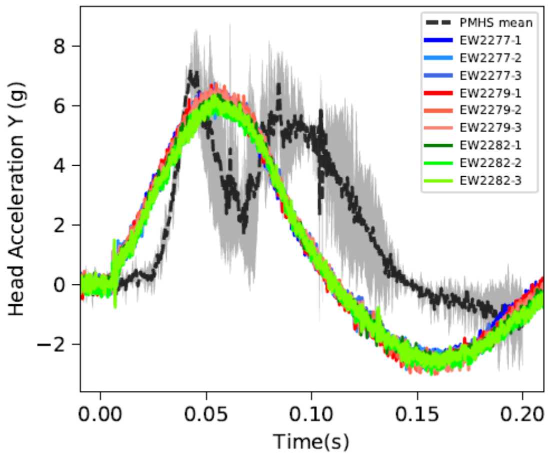

Fig. A26. Head acceleration Y

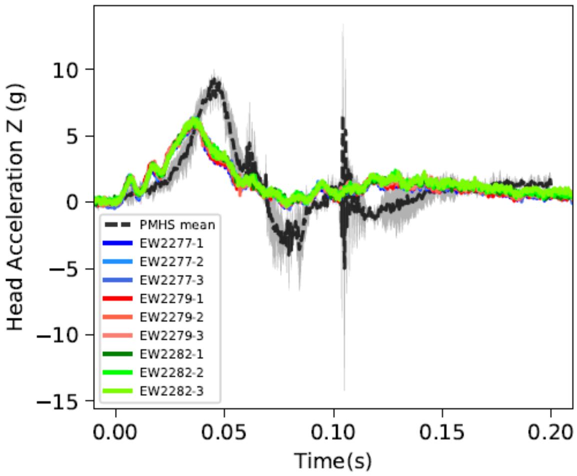

Fig. A27. Head acceleration Z

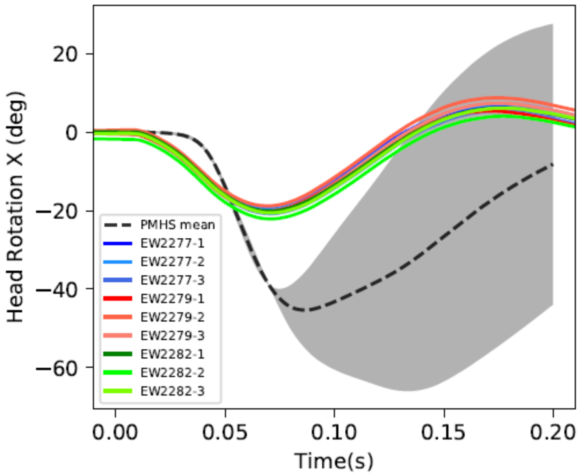

Fig. A28. Head rotation X

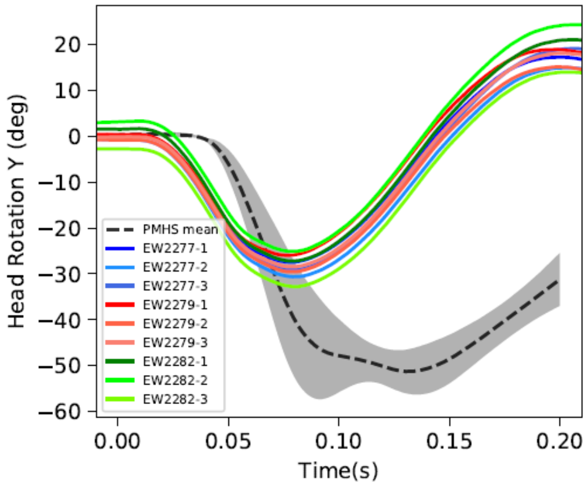

Fig. A29 Head rotation Y

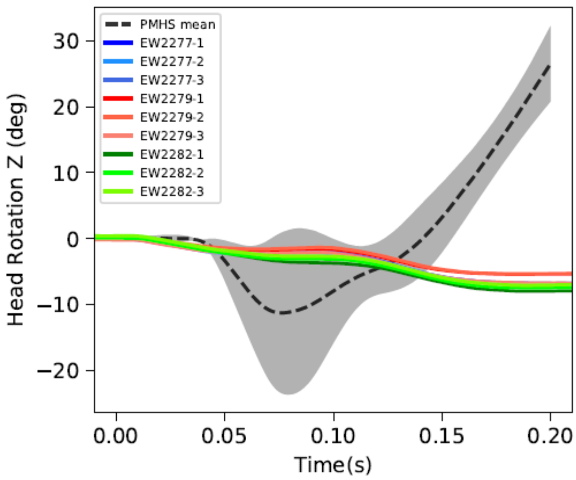

Fig. A30. Head rotation Z

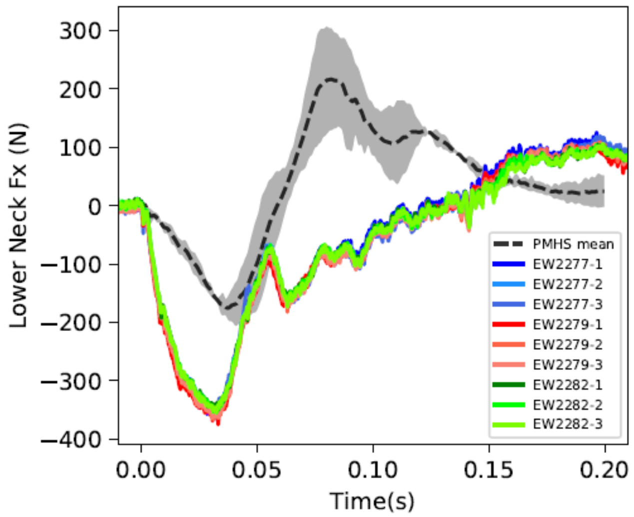

Fig. A31. Lower neck force X

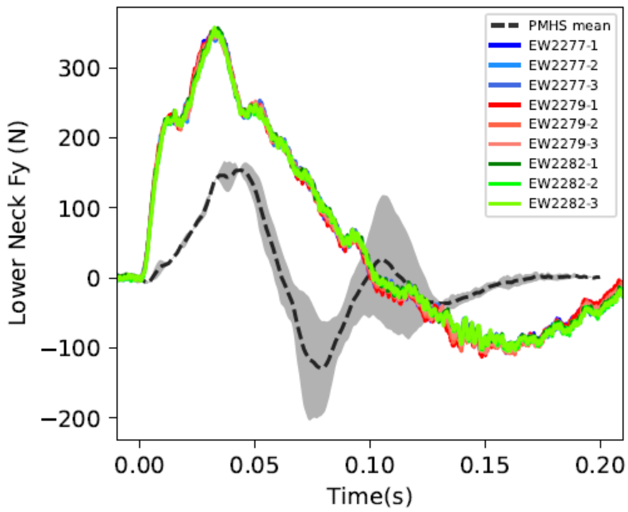

Fig. A32. Lower neck force Y.

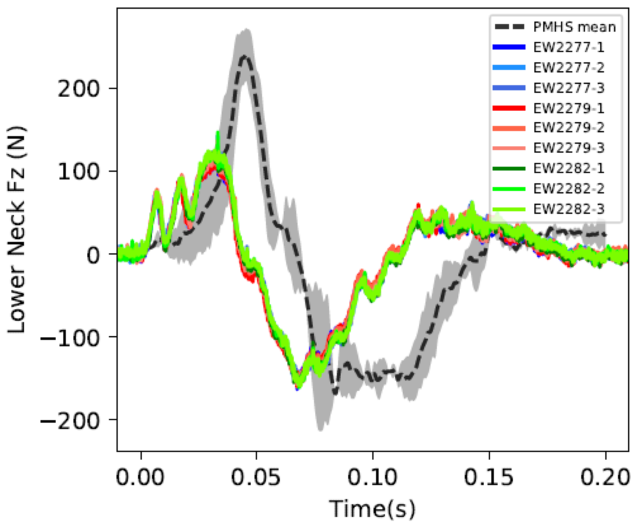

Fig. A33. Lower neck force Z

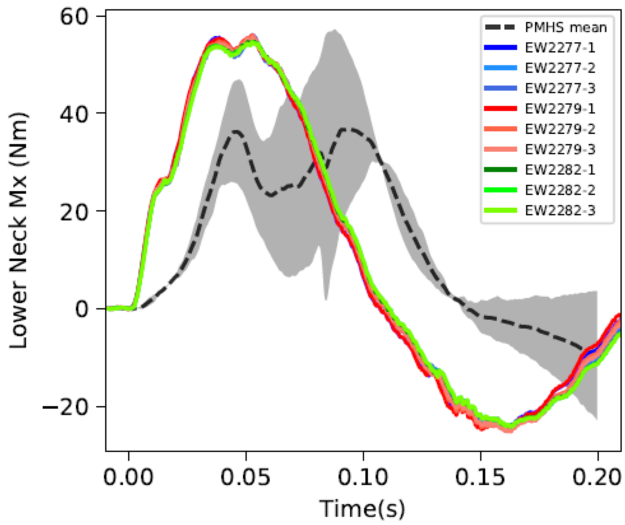

Fig. A34. Lower neck moment X

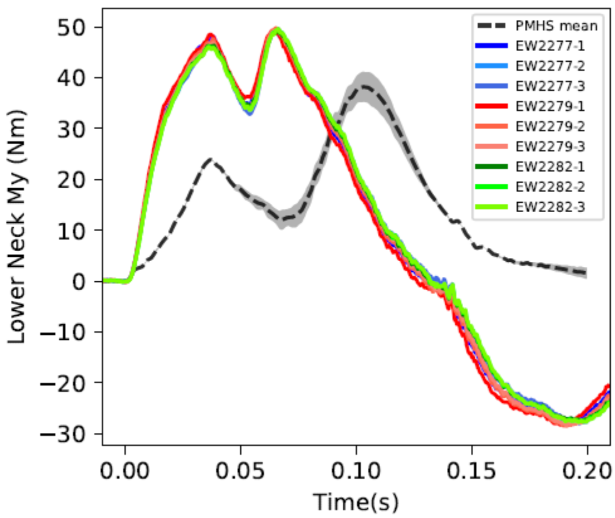

Fig. A35. Lower neck moment Y

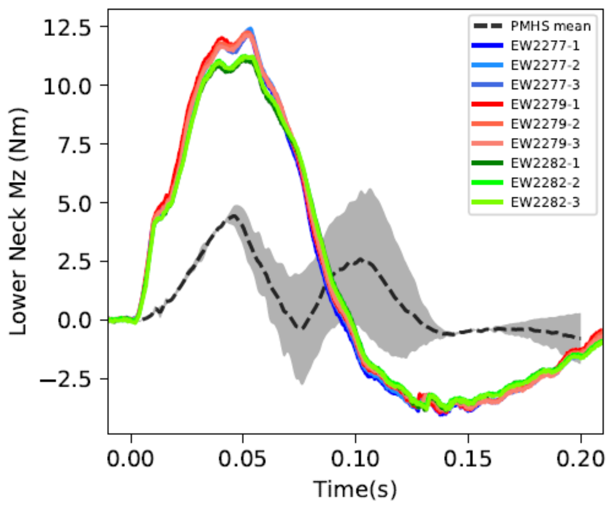

Fig. A36. Lower neck moment Z

Torsion – Kang et al. [6]

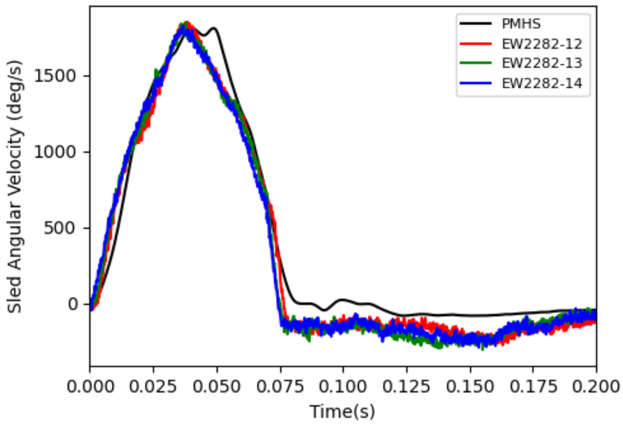

Fig. A37. Sled angular velocity Z

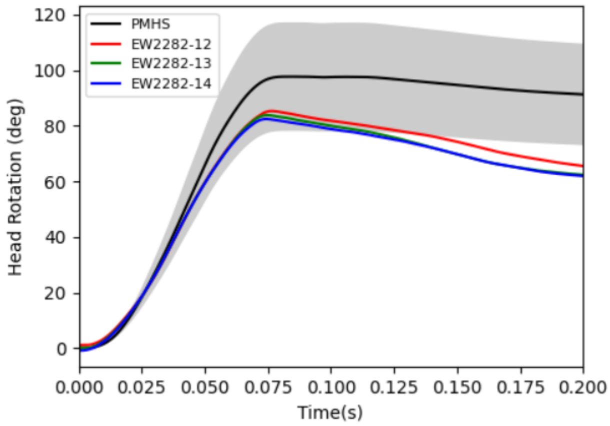

Fig. A38. Head rotation Z

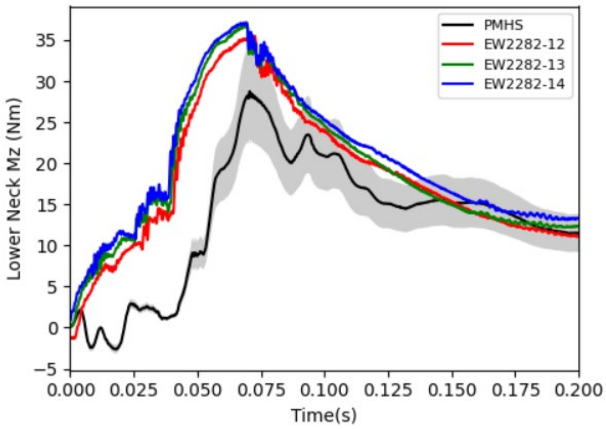

Fig. A39. Lower neck moment Z

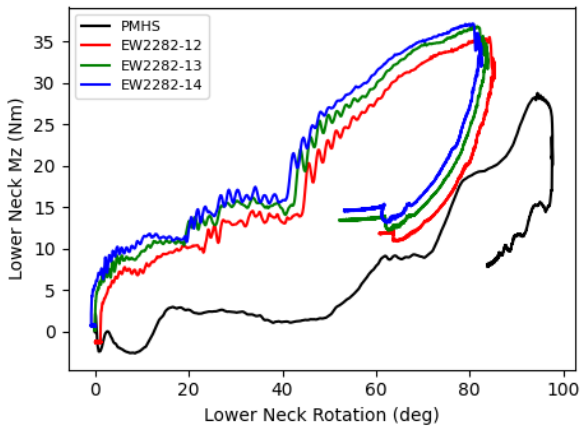

Fig. A40. Lower neck moment Z vs. rotation Z